ICAS 2021 SHANG HAI
International Council of the Aeronautical Sciences
32nd Congress of the International Council of the Aeronautical Sciences
September 6-10, 2021
Pudong Shangri-La, Shanghai, China

COMPUTATIONAL FLUID-STRUCTURE INTERACTIONS OF A 3D FLEXIBLE FLAPPING WING

Yueyang Guo [1], Wenqing Yang [1], Yuanbo Dong [1], Xinyu Lang [1]

[1]School of Aeronautics, Northwestern Polytechnical University, Xi'an, 710072, P. R. China

Abstract

In this paper, we focus on the dynamic mechanical properties of flapping wings with highly flexible structures, which has a structure of anisotropic and batten-enforced, allowing a better understanding of the resulting fluid-structure interactions (FSI). Based on the ANSYS Workbench platform, we developed a three-dimensional (3D) aeroelastic framework for the flapping wing, which has a flexible multibody system subjected to an external incompressible turbulent flow. The Transient Structural module is used to calculate the structural deformation of the flexible wing. The flow field around the flexible wing is calculated in the Fluid Flow (Fluent) module. And the dynamic mesh and overset mesh methods are combined to update the mesh of the fluid domain. The displacement data of the flexible wing is exchanged with the force data in the flow field around it in the System Coupling module. In order to verify the effectiveness of the method, we selected the experimental model in a reference, and compared the calculated results with the experimental results.

Keywords: FSI; ANSYS Workbench; 3D aeroelastic framework; flapping wing

1. Introduction

In recent years, the efficient flight mechanism of flying animals has been widely concerned by scientists and engineers. In fact, one might like to understand these biological systems first, extract certain desirable features, and then apply them to MAV design. However, it is well known that flying animals typically have flexible wings to adapt to the flow environment. Therefore, nature's choice of flexible structures can be put into practice for MAVs.

Understanding the complex fluid-structure interactions due to the flexibility of the animal wing is essential for the development of high-performance and robust MAVs capable of performing desirable missions. When the stiffness distribution and mass distribution of the flapping wing change, the natural frequency and corresponding vibration mode of the structure will change, which will cause the dynamic response of the flapping wing structure to change. And especially when considering the interactions between the structure and the fluid, the aerodynamic characteristics will have significant differences. Through the in-depth study of the relationship between aerodynamic characteristics and structural deformation of wings, it is helpful to provide guidance for the design of flapping wing with high lift, low drag or high thrust.

At present, the numerical model of micro flapping wing flight mainly adopts the method of "rigid wing" simulation, and the flexible structural deformation of the wing is rarely considered in the research. However, the actual flapping wing aircraft pursues the factors of light weight and high efficiency. The wings of the aircraft are constantly thinning. For example, most of the flapping wing aircraft currently use carbon fiber skeleton and membrane skin structure. When it flutters, the structure will be deformed by aerodynamic force, and the vortex structure will change due to the corresponding changes of fluid region, which cannot be ignored[1]. Compared with the flexible fixed wing, the flapping motion of the flexible flapping wing is a large amplitude motion, and the frequency of the structure itself is coupled with the motion frequency and the unsteady aerodynamic force, so it is very difficult to obtain a more accurate solution in the numerical simulation.

According to their own advantages, flapping wing researchers have made exploratory researches on the aerodynamic and structural characteristics of wings, and some preliminary results have been obtained. Through experiments and numerical simulations, they conducted in-depth analysis on the interactions between biological wings in nature or artificial bionic wings and the air during flapping, including chord flexibility[2][3], spanwise flexibility[4][5], spanwise and chordwise coupling of isotropy and anisotropy[6][7][8]. Heathcote et al.[9] carried out experiments on isotropic and chord-like flexible flapping wings under the condition of zero free flow velocity and found that all flexible flapping wings have higher thrust power ratio than rigid flapping wings. Hamamoto et al.[10] analyzed the hovering flight of dragonflies based on the finite element analysis method of arbitrary Lagrange - Euler method. The measured stiffness and mass distribution of dragonfly wings were input into the calculation model by changing the thickness in a certain way. Finally, the section deformation angle of dragonfly hovering flight was very consistent with the actual experimental measurement in the time variation course of one cycle. They also found that the energy consumption of rigid and flexible wings is almost the same, but the peak power of rigid wing is 34% higher than that of flexible wing, which will put forward higher requirements for power supply, actuator and mechanism. Lua et al.[11] obtained a similar conclusion in the experiment of isotropic wing. Based on Ellington's equation[12], Shahzad et al.[13] considered three wing shapes(defined by the radius of the first moment of wing area), with four aspect ratios (AR), and they used a set of flexible wings with two different effective stiffness. Its flapping motion function accords with the motion law of hoverfly, bumblebee, lacewing, and hawkmoth. The 3D, viscous, incompressible Navier–Stokes equations are solved using a sharp interface immersed boundary method, which is strongly coupled with an in-house nonlinear finite element based structural solver for fluid–structure interactions of isotropic and homogeneous flexible wings in hover at a Reynolds number of 400. It is concluded that flexible wings with high AR produce less lift than rigid wings because of lower pitch angles during the mid-stroke, but they are more efficient in terms of power economy.

Based on our previous work and the ANSYS Workbench platform, we proposed a set of fluid-structure coupling calculation process for calculating the wing model (carbon fiber rod + polyester film) used in most flapping wing aircraft, and verified the reliability of the numerical results, and conducted a brief structural analysis and aerodynamic analysis on the calculation results of the flapping wing used in this paper.

2. Computational procedure

2.1 Model

2.1.1 *Wing geometry and mesh generation*

The research object selected in this paper is the flapping wing (Figure 1 (a)) of the “Dove” [14] — A bird-mimetic flapping-wing micro aircraft developed by the Northwest Polytechnic University （NWPU） in China. Since the curvature of the beam and membrane will increase the calculation amount and difficulty, the initial structure of the flapping wing is simplified as straight rod and flat membrane. As shown in Figure 1 (b), the flapping wing skeleton consists of leading-edge beams, oblique beams and wing ribs.

Because this kind of structure type is adopted by most flapping-wing aircraft at present, the research object of this paper has certain universality. For example, RoboBee[15] - a bee like flapping wing aircraft developed by the robot team of Harvard University, Kubeetle[16] - a beetle "Allomyrina dichotoma" like aircraft developed by Konkuk University, Colibri[17] - a hummingbird like hovering flapping twin-wing robot designed by Université libre de Bruxelles and so on.

The simplified Structural finite element model is shown in Figure 1 (c). The beam element is used to model the carbon fiber rod, and either the shell element or solid element can be used to model the polyester film. When the intrinsic properties of the structure and the transient response without considering the interaction with fluid are calculated, the shell element is generally used to model the structure to reduce the amount of computation and improve the efficiency of calculation. However, in the fluid-structure coupling analysis, considering the data transfer of force and displacement between

the surface of polyester film and the fluid, the polyester film is modeled as the solid element to capture local flow characteristics and improve the accuracy data transfer[18].

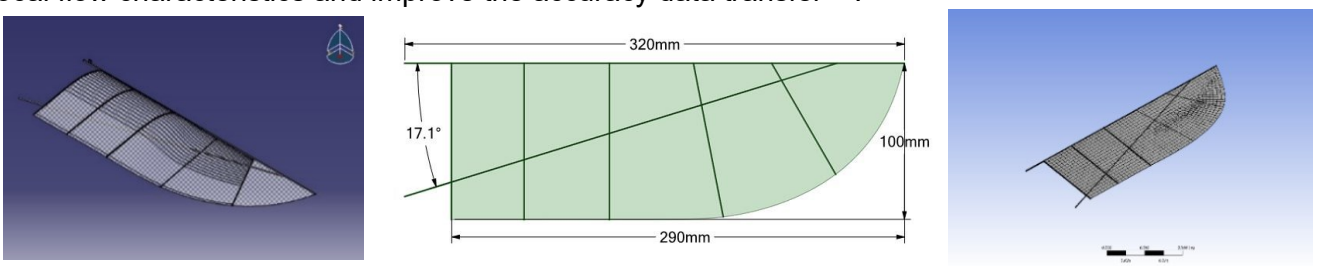

(a) Original model (b) Simplified model (c) Mesh (Structural)

Figure 1 - 3D digital model of flapping wing structure of the “Dove”.

Figure 2 (a) shows the mesh of fluid region in the initial state of wing flutter (the wing is at the beginning of downward stroke or at the end of upward stroke). The technique of overset mesh is adopted in the mesh generation, and the cell around the wing is wrapped by the component mesh as shown in. The overset boundary moves in the same flapping motion as the wing root, so that it less likely to cause negative cell volume in the mesh due to large angular changes. The internal of component mesh (fluid mesh deformation due to wing shape deformation) is stretched by the technique of Dynamic mesh (diffusion), which can better ensure the mesh quality near the wing after deformation. To save computing resources and time, half of the fluid model is used, the boundary of symmetry is used in the middle of the background grid, and the size of the external flow field is "45c × 30c × 15c".In the absence of incoming flow, the approximate Reynolds number of the wing flapping motion is 80,000, so it is calculated that the thickness of the first boundary layer is set as 2×10^{-4}c, and the number of layers is 20. The component mesh and the background mesh near the wing are unstructured mesh, and the total amount of fluid mesh is about 4.2 million.

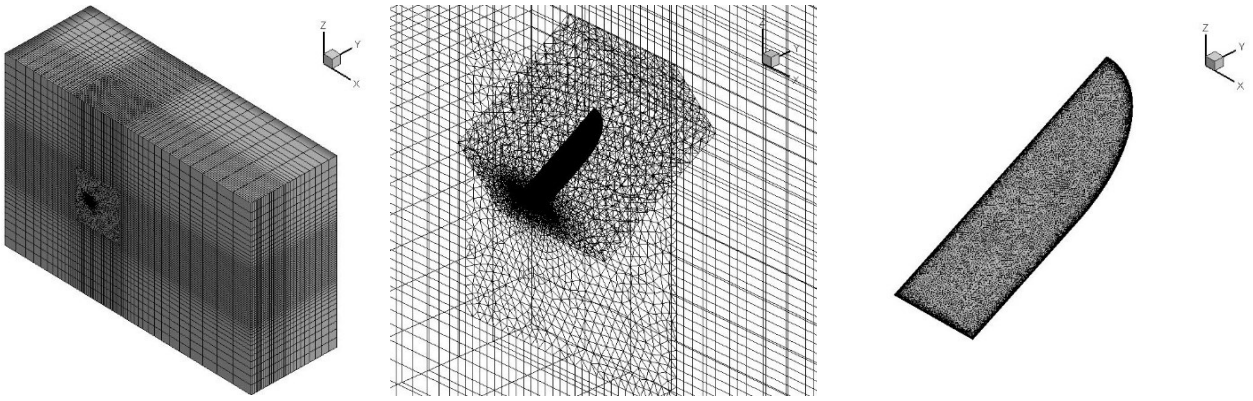

(a) Assembled mesh (b) Component mesh (c) Mesh of wing surface (Fluid)

Figure 2 - Overset mesh system in flapping airfoil simulation.

2.1.2 *Wing flexibility parameters and flapping kinematics*

The wing rod of “Dove” flapping wing aircraft is modeled by beam element, and the membrane is modeled by solid or shell element. The two material parameters used are shown in Table 1. The flapping function in the numerical simulation refers to the “Dove” flapping wing aircraft. The flapping frequency is 10Hz and the amplitude is 30 ° simple harmonic motion of flapping.

Table 1 - Material properties of flexible wings.

Element	Material	Density(kg/m^3)	Young’s Modulus(Pa)
Beam	Carbon fiber rod	130	2×10^7
Shell/solid	Polyester film	1750	1.2×10^{11}

It is worth noting that although the seven carbon rods on the “Dove” wing have the same material parameters and solid cylindrical section, they have different section sizes. As shown in Figure 3, the

orange beam corresponds to the carbon rod with a diameter of 2mm, the blue inclined beam corresponds to the carbon rod with a diameter of 1.5mm, and the two green beams at the wing tip corresponds to a diameter of 1mm. And the thickness of the Shell/Solid is 0.4mm.

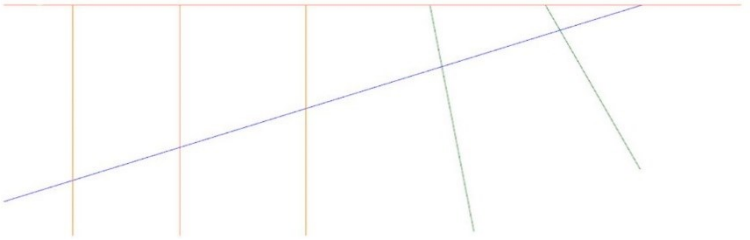

Figure 3 – Beams of flapping wing structure of the “Dove”. (Orange:2mm, Blue:1.5mm, Green:1mm).

2.1.3 *Performance parameters*

This paper mainly introduces the fluid structure coupling analysis process of a three-dimensional flapping wing on the ANSYS Workbench platform, and only makes a brief analysis of its structural performance and aerodynamic performance. To verify the reliability of the analysis process results, referring to the experimental data of Heathcote et al.[9], we have used the time histories of trust coefficient(C_T), and calculated the lift coefficient (C_L) for the results of the flexible wing in this paper in Eq. (1), and the values of these coefficients are obtained in the fourth and fifth flutter flapping cycle. Where F_L and F_T is the vertical and horizontal component of the resultant force, and U is the reference velocity (Incoming flow velocity - example verification; The average velocity of the wingtip -flapping wing analysis in this paper). The S is the projected area of the wing surface, ρ_f is the reference density of the fluid.

$$C_L = \frac{F_L}{(1/2)\rho_f U^2 S};\ C_T = \frac{F_T}{(1/2)\rho_f U^2 S} \tag{1}$$

In the structure module, we use frequency ratios(Ratio of flapping frequency to the first order natural frequency of the structure) , the bending deformation and torsion deformation to make a rough analysis of this structure.

2.2 Computational solver

The workflow for two-way FSI simulation on the ANSYS Workbench platform[19] is shown in Figure 4. In this flowchart, the Transient Structural module is used to calculate the structural deformation of the flexible wing. The bars are modeled as beams, which are mainly used to withstand bending moments, increase the stiffness of the flexible wing and transmit motion at the same time. A flat 3D wing is modeled as a plate capable of bearing aerodynamic loads and that allows for spanwise bending and chordwise twist. The flapping wing only has a simple single-degree-of-freedom flapping motion. The flow field around the flexible wing is calculated in the Fluid Flow (fluent) module consists of a three-dimensional fluid solver with a RANS model. And the dynamic mesh and overset mesh methods are combined to update the mesh of the fluid domain. The displacement data of the flexible wing is exchanged with the force data in the flow field around it in the System Coupling module. In the actual forward flight of the flapping wing micro aircraft, a specific flight state is selected. By changing such parameters as beam section shape, section size and beam position distribution in the plane to change the stiffness distribution and mass distribution, with the natural frequency of the structure and the corresponding vibration mode as the measurement, to study the relationship between the aerodynamic force, power consumption characteristics of the flapping wing and the frequency ratio, the natural mode. Aerodynamic force and power consumption are combined to evaluate the aerodynamic efficiency of flexible wing structures. From the aspects of flexible deformation and flow field structure of the wing, the effect mechanism of the fluid-structure interactions of the three-dimensional anisotropic flexible flapping wing is revealed.

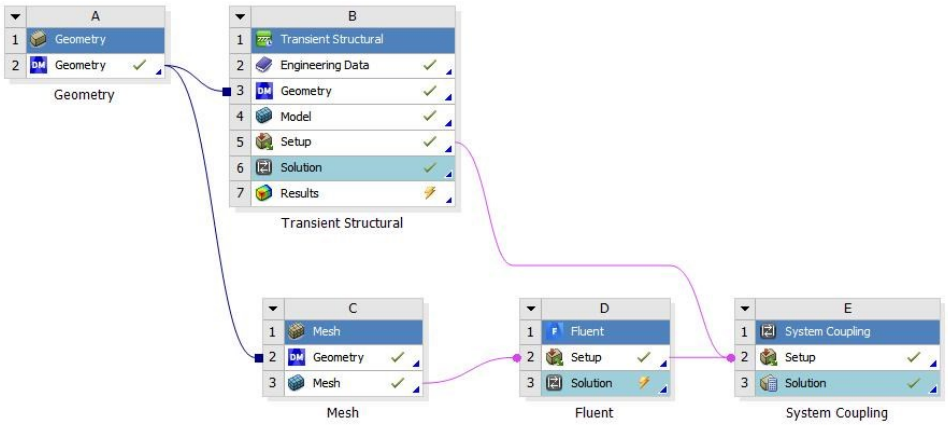

Figure 4 - Screenshot from ANSYS Workbench showing a workflow for FSI.

2.3 Solver validation

2.3.1 *Structure solver verification*

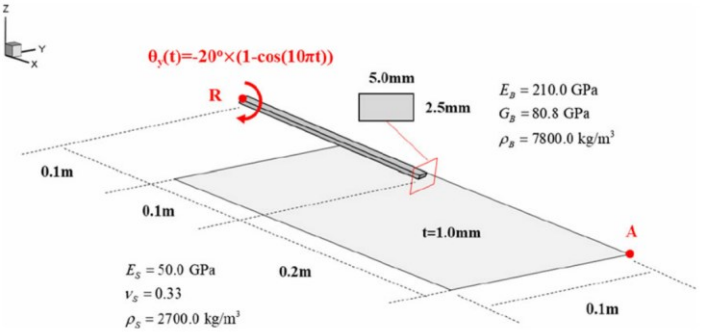

(a) Analysis condition and configuration of a beam/shell combined structure.

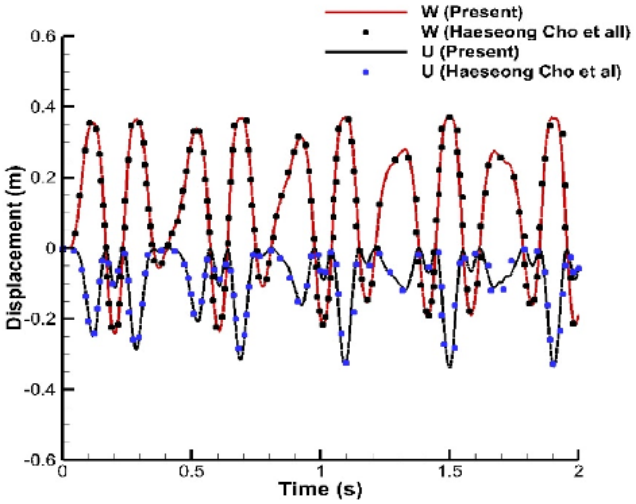

(b) Displacement history at Stations A of a beam/shell combined structure
U - The displacement in the X direction; W - The displacement in the Z direction

Figure 5 - Verification of the structural solver.

To verify the rationality and effectiveness of the structural nonlinear solver, we choose to compare the calculation results of Cho et al.[20]. As shown in Figure 5 (a), the calculation model consists of a beam and a shell with a simple harmonic flapping motion with a flapping amplitude of 20 degree and a flapping frequency of 5 Hz. Figure 5 (b) shows the displacement of the wingtip point A, which is the result of our calculation (solid line) and the result of Cho et al.[20] (discrete points). The present analysis shows good correlation with their prediction.

2.3.2 *Verification of fluid structure coupling solver*

To verify the effectiveness of the method, we selected the experimental model in the reference, namely the three-dimensional wing model with high stiffness and plunging motion[9], to carry out the calculation and compared the calculated results with the experimental results.

As shown in Figure 6(a), it is the experimental measurement device of Heathcote et al.[9]. In their experiments, three flat wings with the same cross-section shape and different cross-section structures were selected (representing inflexible, flexible and highly flexible respectively, as shown in Figure 6(b)). Figure 6(c) is shown the schematic of the spanwise flexible wing heaving periodically.

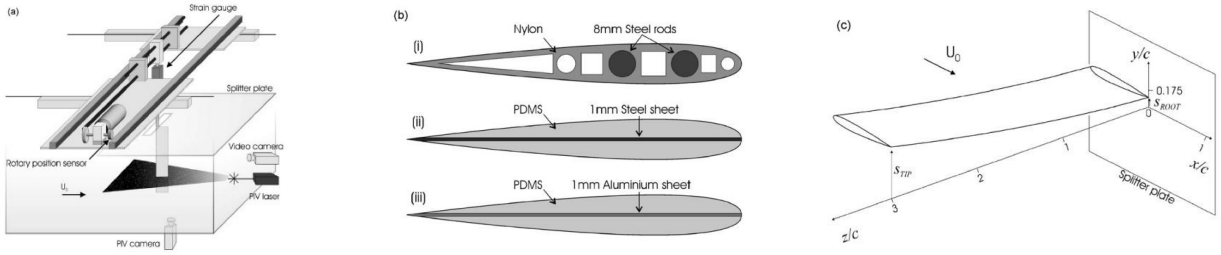

(a)Water tunnel experimental set-up for force measurements

(b)Cross-sections of the three NACA0012 wings

(c)Schematic of the spanwise flexible wing

Figure 6 - Experimental setup in Heathcote et al.'s experiment.

In this paper, the flexible wing(Figure 6(b)(ii)) is selected as an example for verification. In the experiment, it is made of polydimethylsiloxane rubber (PDMS) cast in NACA0012 mold, reinforced with 1 mm stainless steel plate in the middle. We divided it into three areas in the computer for modeling (upper, middle and lower respectively), combined them by method of "Bonded" on the platform of ANSYS Mechanical, and meshed them. The result is shown in Figure 6, with a mesh amount of about 300,000.

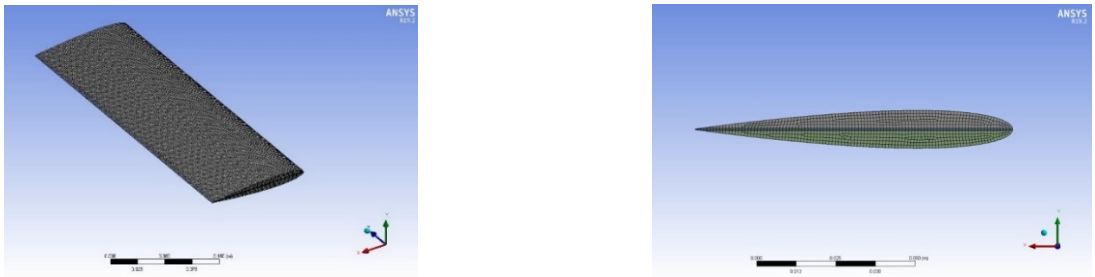

Figure 7 – Structural mesh model of 3D flexible wing with high stiffness and plunging motion.

The parameters used in this simulation are presented in Table 2. The fluid parameters, such as chord length, half-span length, and Amplitude of plunging were given in the experimental report of Heathcote et al[9], and the structural parameters referred to the material properties of real steel and PDMS materials.

Table 2 - Numerical simulation parameters of flexible wing with high stiffness and plunging motion.

Fluid parameters	Value
Chord length (c)	0.1 m
Half span (b)	0.3 m
inlet velocity (U)	0.3 m/s
Fluid density (ρ_f)	10^3 kg/m^3(Water)
Amplitude of plunging (A)	0.0175 m
Reynolds number (Re)	3×10^4
Reduced frequency (k)	1.82
Strouhal number (St)	0.202

Structural material parameters		Value
Steel	Density	7850 kg/m^3
	Young's Modulus	2.1×10^5 MPa
	Poisson's Ratio	0.3
PDMS	Density	
	Young's Modulus	0.25 MPa
	Poisson's Ratio	0.49

The Comparison of results is shown in Figure 8.The curve of the thrust coefficient(Figure 8(a)) and the curve of the wingtip displacement(Figure 8(b)) with the time course of the flexible wing are presented respectively. It can be seen that the wingtip displacement curve (black solid line) obtained according to the above calculation process can match well with the experimental value (red discrete points), but there is a gap between the thrust coefficient curve (black solid line) and the experimental value (red

discrete points). We refers to the work of Lee et al.[21] and believes that the wall effect caused by the surrounding walls cannot be ignored when the flat flexible wing with half span of 0.3m and chord length of 0.1m is in a water tank of "0.381m×0.5m×1.5m", which is the numerical simulation of the experiment of Heathcote et al.[9]. Therefore, the flow field area around the flapping wing is rebuilt according to the real water tank size, and the surrounding walls are set as the boundary condition "no-slip wall". The finally obtained thrust coefficient curve is shown by the purple line. Its error relative to the measured value is much smaller and better close to the experimental value. We speculate that the error that still exists in the end is mainly due to the setting of the difference of material model. It also includes that the material model in the numerical simulation cannot perfectly match the material properties of the real world, and of course there are errors in the experimental measurement. The wingtip displacement curve calculated by re-modeling has no obvious change from the previous calculation, so it is not shown. This proves that the fluid structure coupling process is reasonable and effective, only because at the beginning of our computer simulation of real-world experimental data, we failed to set the physical boundary conditions as close to the experimental environment as possible on the basis of ensuring the amount of calculation.

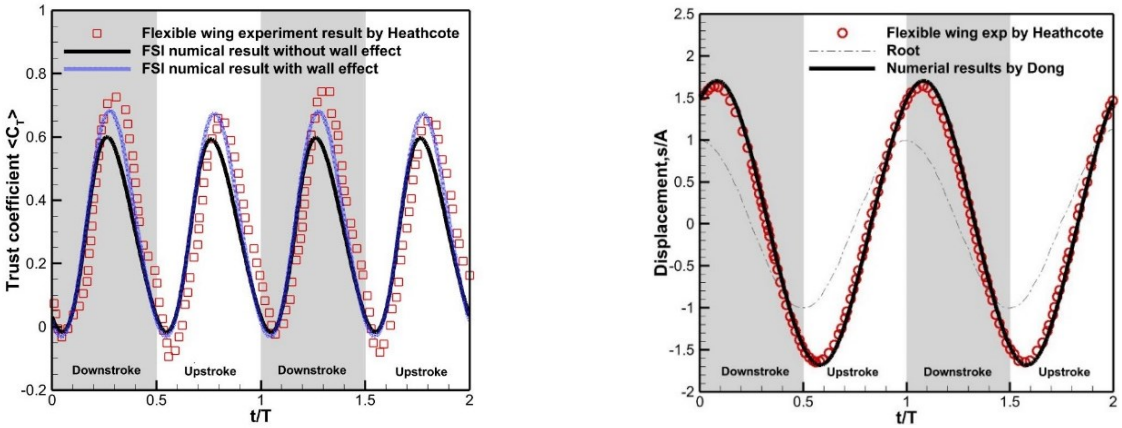

(a)Trust coefficient (b) Tip displacement

Figure 8 - Comparison of numerical calculation results and experimental results.

3. Results

3.1 Modal analysis results

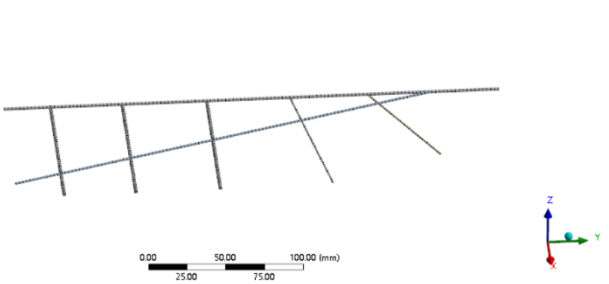

(a) Flapping wing skeleton

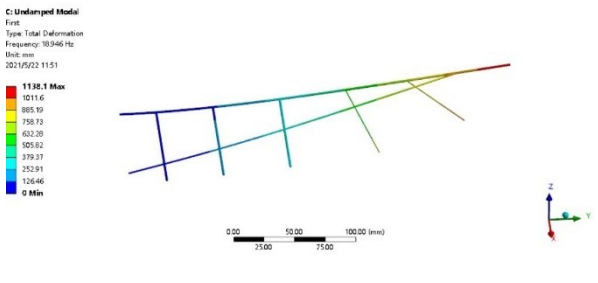

(b) First order natural mode

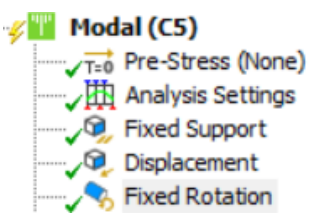

(c) Constrained boundary

	Mode	Frequency [Hz]
1	1.	18.946
2	2.	82.003
3	3.	142.43
4	4.	183.01
5	5.	187.6
6	6.	209.38

(d) Mode frequency

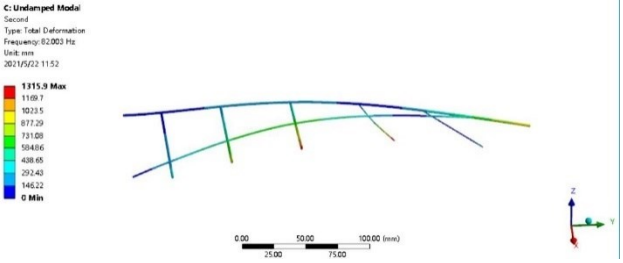

(e) Second order natural mode

Figure 9 - The finite element model of the flapping wing skeleton and its first two natural modes.

The structure is usually further simplified to calculate the deformation characteristics of the structure under different frequency ratios. As shown in Figure 1, due to the small stiffness and large mass of polyester film, the structure has many low-frequency natural frequencies, so the effect of polyester film is ignored in the analysis to analyze the influence of frequency ration on the deformation of the flapping wing skeleton(The effect of air is not considered).As shown in Figure 9, the geometry of the flapping wing skeleton neglecting polyester film, the value of its low-order 6-order natural frequency and the setting of constraint conditions in modal analysis (two points at the root of the wing are fixed, and the point near the trailing edge of the root of the wing does not limit its rotation in the flapping direction), and the geometric schematic diagram of its first and second-order vibration modes are also presented. The frequency ratio (the ratio of the motion frequency of the wing to the first natural frequency of the structure) is widely proved to be an important nondimensional parameter of the flexible flapping wing[22]. The natural frequency obtained by modal analysis can be changed by setting different structures and flapping frequencies to carry out the follow-up research.

3.2 Aerodynamic solution results(Wing - Rigid body)

Before the fluid structure coupling simulation, we calculate the unsteady flow field of the rigid flapping wing in the fluent fluid module. In order to verify the correctness of the fluid module setting and the quality of the fluid mesh (whether there are too many orphan grids in the process of overset mesh interpolation when the component mesh is moving, which affects the accuracy of the calculation), the results of the rigid wing can also be compared with the results of the flexible wing. As shown in Figure 10, under the condition of 10 Hz frequency in the air with an incoming flow velocity of 10m/s, the lift coefficient and drag coefficient of a three-dimensional flapping rigid wing change with time in one cycle. During the movement, the contour maps of pressure coefficient distribution of the wing at three typical positions are shown in Figure 11. The aerodynamic force of the rigid wing and its surrounding flow field structure are calculated by using this method. This method will be combined with the dynamic grid technology to calculate and study the fluid module in the fluid structure interaction of flexible flapping wing.

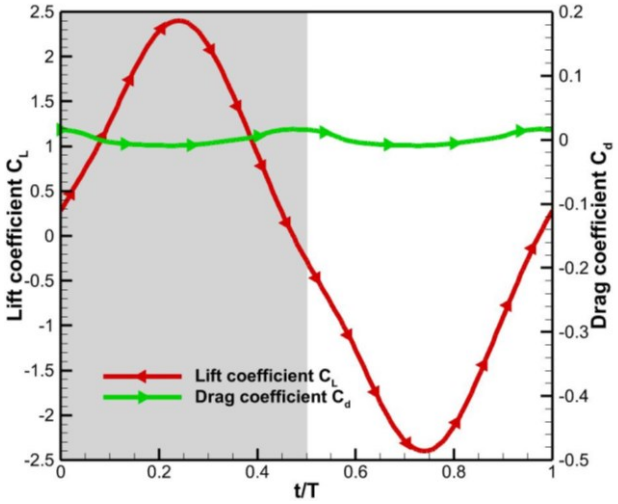

Figure 10 - Force coefficient curve within one period.

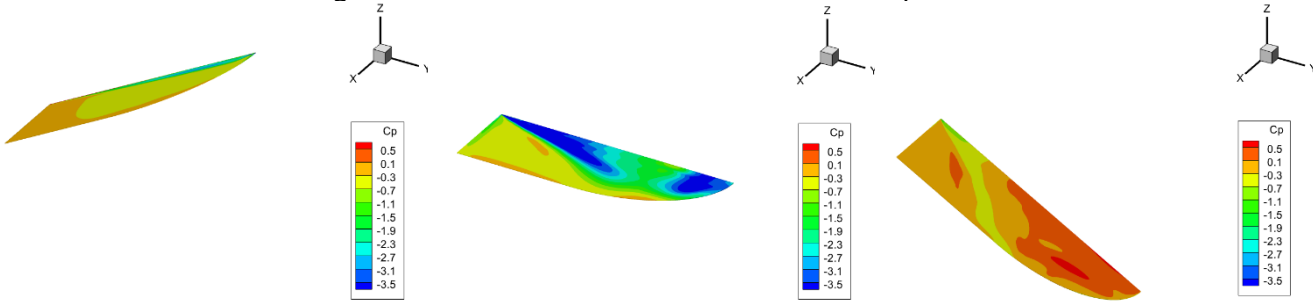

Figure 11 - The contour maps of pressure coefficient distribution of the wing at three typical positions.

3.3 The results of fluid-structure coupling

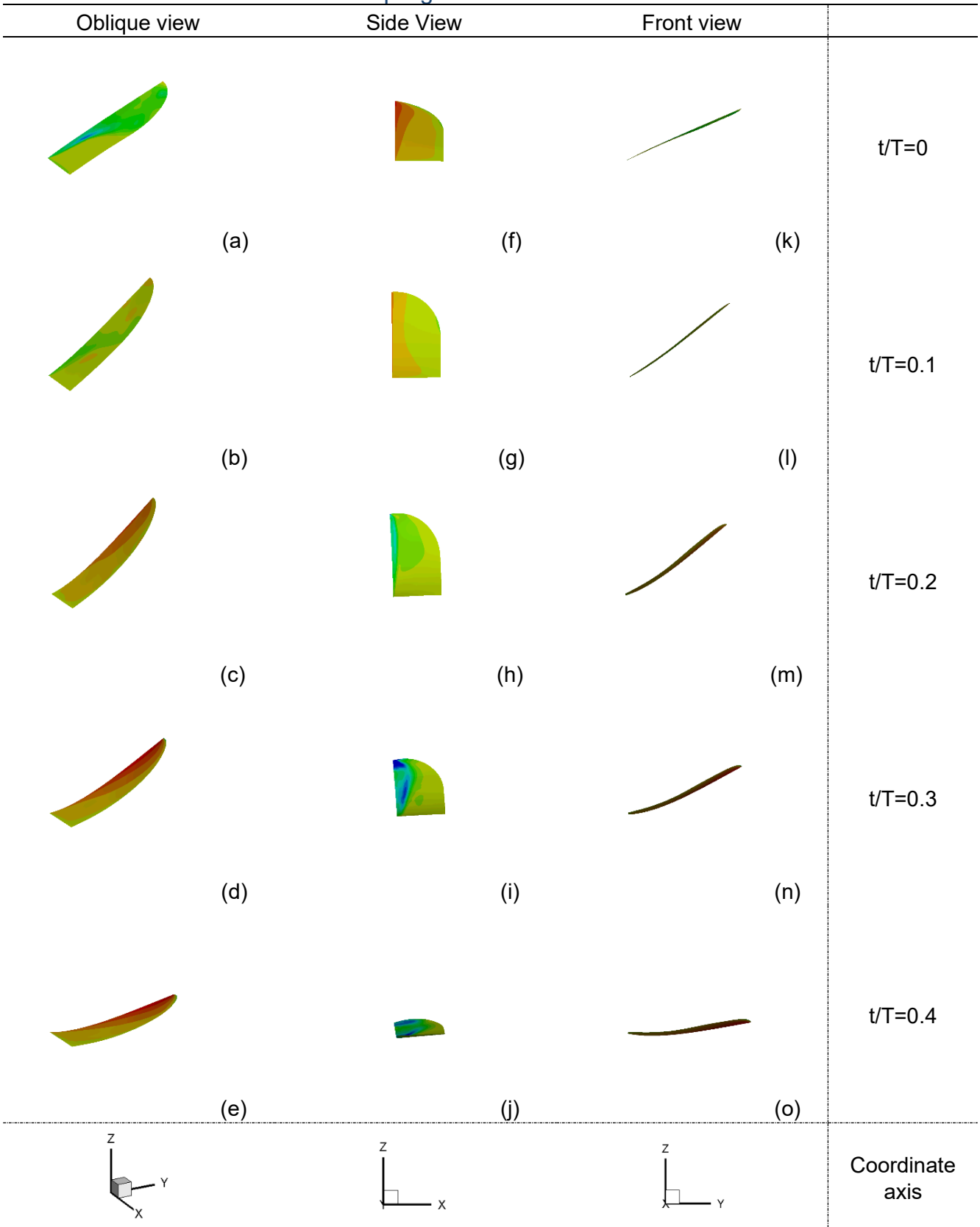

Figure 12 – Pressure contour of five moments in a cycle of the downstroke phase.

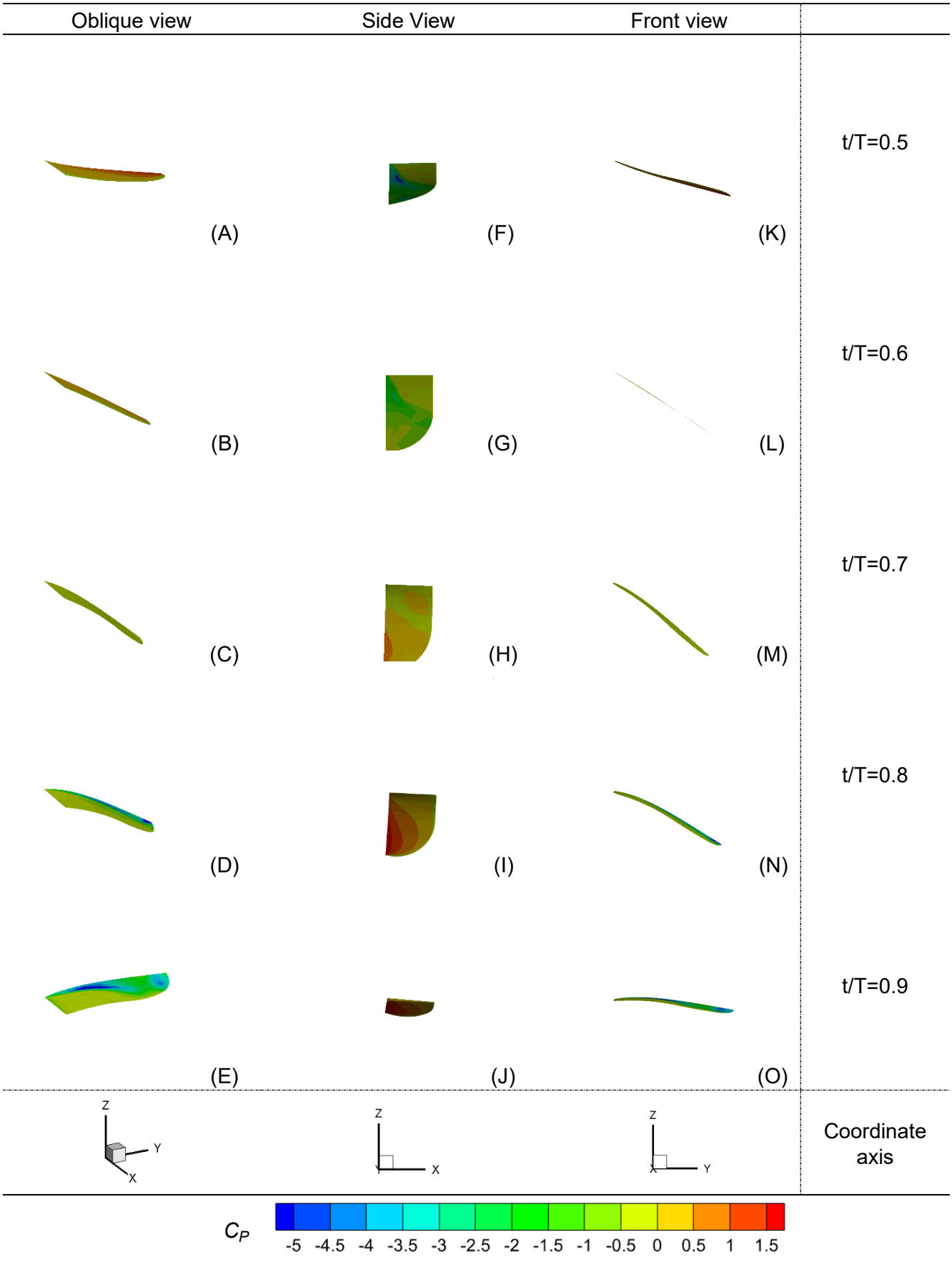

Figure 13 – Pressure contour of five moments in a cycle of the upstroke phase.

Following the separate analysis of structure and fluid to flapping wing above, the method of combining dynamic mesh and overset mesh is used to establish the fluid-structure coupling correspondence relationship of flapping wing surface in the System coupling module (the deformation data of the wing surface is transferred by the structure module, and the movement of the overset mesh is controlled by Fluent UDF with given rigid motion to prevent the large distortion of the mesh near the wing surface from causing negative volume). In this paper, the combination of moving mesh and overset mesh can effectively solve the mesh updating problem of large deformation flexible wing in large flapping motion in three-dimensional unsteady flow field calculation. Figure 12 and Figure 13 respectively show the deformation state at five moments in a cycle of up and down stroke through oblique view, front view and side view (the color on the wing surface corresponds to the corresponding pressure coefficient). It can be seen that the pressure at the leading edge is significantly higher than that at the trailing edge in the forward flight state. And it can also be seen from this series of figures that the wing surface not only has bending deformation, but also has torsional deformation. The causes of bending and torsional deformation will be explored in further detail in future work. Figure 14 shows the time-varying curve of the wingtip in three directions. In the forward flight state, there is a non-negligible torsional deformation, which can be seen from the change curve in the x direction. As shown in Figure 15, the variation curve of the lift resistance coefficient of the flexible wing within a period can be seen that, when the stroke plane is perpendicular to the direction of incoming flow, compared with the rigid wing(Figure 10), the flexible wing has slightly smaller lift coefficient and larger trust coefficient (Negative drag coefficient). With an incoming flow of 10m/s, the flexible wing has forward acceleration under such flapping conditions.

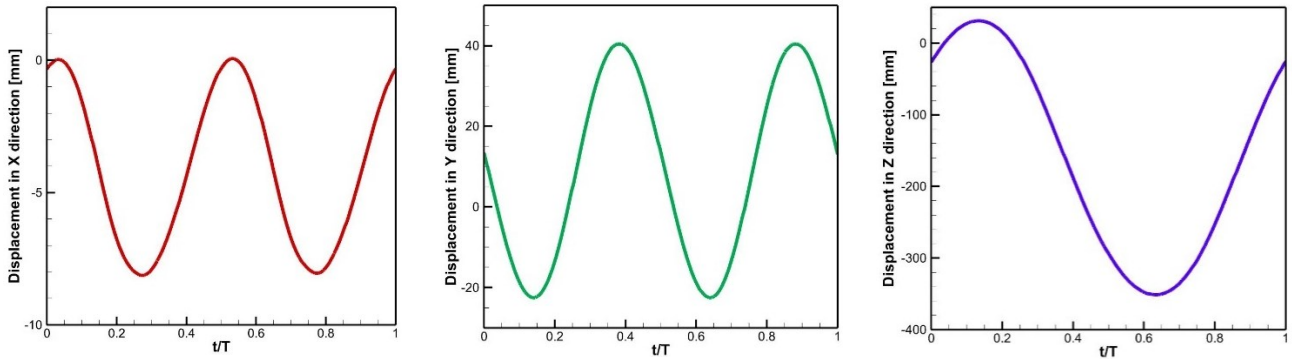

(a) X - direction (b) Y - direction (c) Z - direction

Figure 14 – Tip displacement in three directions

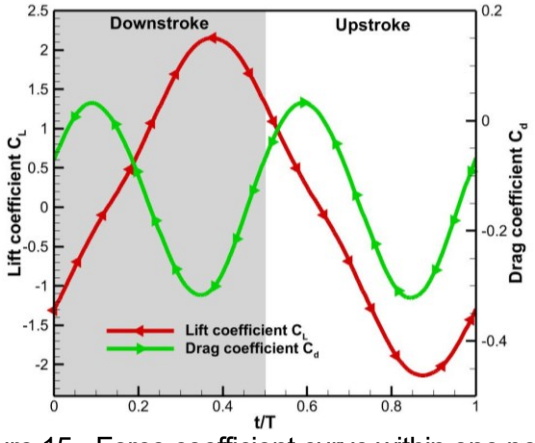

Figure 15 - Force coefficient curve within one period

4. Conclusions

In this paper, a FSI analysis method based on ANSYS Workbench for flexible flapping wings with carbon rod and membrane structure is introduced. We compare the experimental results in references with the results calculated by this numerical method, and they are in good agreement, which proves the effectiveness and rationality of the solution process. The low order natural frequency and mode shape of the skeleton are calculated in the structural module. In the fluid module, the results of rigid flapping

wing are calculated, and the quality of overset mesh interpolation is checked. Finally, the fluid structure coupling analysis is carried out. The deformation state and pressure contour map of flapping wing in three directions and ten moments in a cycle are shown. Based on this work, we will further explore the influence of the frequency ratio of the flapping wing structure motion on the aerodynamic efficiency of the flapping wing in the future and expect of obtaining their inner influence relationship.

5. Contact Author Email Address

Mailto: steamer@mail.nwpu.edu.cn

6. Copyright Statement

7. Acknowledgments

This study was supported by the National Natural Science Foundation of China (11872314) and the Key R&D Program in Shaanxi Province of China (2020GY-154).

References

[1] Prapamonthon P, Yin B, Yang G, et al. Recent progress in flexibility effects on wing aerodynamics and acoustics[J]. *Proceedings of the Institution of Mechanical Engineers*, Part C: Journal of Mechanical Engineering Science, 2020.

[2] Miao J M, Ho M H. Effect of flexure on aerodynamic propulsive efficiency of flapping flexible airfoil[J]. *Journal of Fluids and Structures*, 2006, 22(3): 401-419.

[3] Pederzani J, Haj-Hariri H. Numerical analysis of heaving flexible airfoils in a viscous flow[J]. *AIAA journal*, 2006, 44(11): 2773-2779.

[4] Heathcote S, Wang Z, Gursul I. Effect of spanwise flexibility on flapping wing propulsion[J]. *Journal of Fluids and Structures*, 2008, 24(2): 183-199.

[5] Zhu Q. Numerical simulation of a flapping foil with chordwise or spanwise flexibility[J]. *AIAA journal*, 2007, 45(10): 2448-2457.

[6] Young J, Walker S M, Bomphrey R J, et al. Details of insect wing design and deformation enhance aerodynamic function and flight efficiency[J]. *Science*, 2009, 325(5947): 1549-1552.

[7] Agrawal A, Agrawal S K. Design of bio-inspired flexible wings for flapping-wing micro-sized air vehicle applications[J]. *Advanced Robotics*, 2009, 23(7-8): 979-1002.

[8] Aono H, Chimakurthi S K, Wu P, et al. A Computational and experimental studies of flexible wing Aerodynamics[C]//*48th AIAA aerospace sciences meeting including the new horizons forum and aerospace exposition*. 2010: 554.

[9] Heathcote S, Gursul I. Flexible flapping airfoil propulsion at low Reynolds numbers[J]. *AIAA journal*, 2007, 45(5): 1066-1079.

[10] Hamamoto M, Ohta Y, Hara K, et al. Application of fluid–structure interaction analysis to flapping flight of insects with deformable wings[J]. *Advanced Robotics*, 2007, 21(1-2): 1-21.

[11] Lua K B, Lai K C, Lim T T, et al. On the aerodynamic characteristics of hovering rigid and flexible hawkmoth-like wings[J]. *Experiments in fluids*, 2010, 49(6): 1263-1291

[12] Ellington C P. The aerodynamics of hovering insect flight. II. Morphological parameters[J]. *Philosophical Transactions of the Royal Society of London. B, Biological Sciences*, 1984, 305(1122): 17-40.

[13] Shahzad A, Tian F B, Young J, et al. Effects of flexibility on the hovering performance of flapping wings with different shapes and aspect ratios[J]. *Journal of Fluids and Structures*, 2018, 81: 69-96.

[14] Xuan Jianlin, Song Bifeng, Song Wenping, et al. Progress of Chinese “Dove” and future studies on flight mechanism of birds and application system [J].*Transactions of Nanjing University of Aeronautics and Astronautics*,2020,37(05):663-675.

[15] Breuer K. Flight of the RoboBee[J]. Nature, 2019, 570(7762): 448-449.

[16] Phan H V, Aurecianus S, Kang T, et al. KUBeetle-S: An insect-like, tailless, hover-capable robot that can fly with a low-torque control mechanism[J]. *International Journal of Micro Air Vehicles*, 2019, 11.

[17] Roshanbin A, Altartouri H, Karásek M, et al. COLIBRI: A hovering flapping twin-wing robot[J]. *International Journal of Micro Air Vehicles*, 2017, 9(4): 270-282.

[18] Banerjee B, Chen Z, Das R, et al. Comparison of ANSYS elements SHELL181 and SOLSH190[J]. 2011.

[19] Chimakurthi S K, Reuss S, Tooley M, et al. ANSYS Workbench System Coupling: a state-of-the-art computational framework for analyzing multiphysics problems[J]. *Engineering with Computers*, 2018, 34(2): 385-411.

[20] Cho H, Gong D H, Lee N, et al. Combined co-rotational beam/shell elements for fluid–structure interaction analysis of insect-like flapping wing[J]. *Nonlinear Dynamics*, 2019, 97(1): 203-224.

[21] Lee N , Lee S , Cho H , et al. A computational study of wall effects on the aeroelastic behavior of spanwise flexible wings[J]. *International Journal of Aeronautical & Space Sciences*, 2019.

[22] Shyy W, Aono H, Kang C, et al. *An introduction to flapping wing aerodynamics*[M]. Cambridge University Press, 2013.